Asian Journal of Chemistry; Vol. 36, No. 5 (2024), 1151-1160

ASIAN JOURNAL OF CHEMISTRY

https://doi.org/10.14233/ajchem.2024.30995

Synthesis, Characterization of ZnO-based Nanocomposites and its Effect on the Viscosity of Gasoline Engine Lubricating Oil

SADANANDA[1], GLADSON FRANCIS CRASTA[1], R. DIVYA[1], SUMANTH SHETTY[1], M. NAGALAKSHMEE[1], D.M. MANJESH[1], DINESH RANGAPPA[1,*] and MANJUNATH SHETTY[2,*]

[1]Department of Applied Sciences (Nanoscience and Technology), Centre for Post-Graduate Studies, Visvesvaraya Technological University, Muddenahalli Campus, Chikkaballapur-562101, India
[2]Department of Aeronautical and Automobile Engineering, Manipal Institute of Technology, Manipal Academy Higher Education, Manipal-576104, India

*Corresponding authors: E-mail: dineshrangappa@gmail.com; manjunath.shetty@manipal.edu

Received: 2 December 2023; *Accepted*: 3 April 2024; *Published online*: 30 April 2024; AJC-21622

This study represents the synthesis, characterization of ZnO nanoparticles and encapsulated composites with MWCNT, sodium dodecyl sulfate (SDS) and cetyltrimethylammonium bromide (CTAB) for the lubricating performance in petrol engine oil. The facile sol-gel process was used to synthesize ZnO and ZnO-based nanocomposites followed by annealing at 500 ºC. ZnO-based nanocomposite samples were prepared by adding different secondary encapsulating agents such as MWCNT (with different wt.% of 1, 2 and 3), SDS and CTAB. The as-synthesized ZnO and ZnO-based nanocomposite samples were further dispersed in 20W40 grade engine oil separately by taking 50 mL volume of oil. Different amounts of the synthesized samples of 50 mg, 100 mg and 150 mg were blended with the lubricant accordingly by the sonication process. After that the viscosity performances were carried out for all the prepared samples. The dynamic and kinematic viscosity were measured using a redwood viscometer and the temperature varied throughout the analysis at 34, 44 and 55 ºC to observe the optimum temperature effect on viscosity performance. The objective of this work is to determine the temperature effects on the viscosity of commercial lubricant 20W40 grade by blending with different suspended novel nanomaterials.

Keywords: Petrol engine lubricant, Multi-walled carbon nanotube, Sodium dodecyl sulfate, Cetyltrimethylammonium bromide.

INTRODUCTION

In automobiles, during the transformation of heat energy into mechanical energy by burning of fuel, transmission systems play a crucial role. In this regard, engine efficiency depends on the effective utilization of energy stored in the fuel. Some major issues in automobiles related to reduced engine efficiency are increased fuel consumption, more oil consumption, engine overheating and excessive engine noise, *etc*. [1-3]. The primary problem with power transmission system is friction [4,5]. One of the most important key factors influencing engine performance, is the friction between two moving components which may lead to high fuel consumption, poor engine power output, high exhaust emissions and hence, require more maintenance and a shorter engine life [6]. Improving fuel efficiency by reducing friction has been one of the most serious challenges confronting the vehicle industry. The possibility to reformulate the lubricating oil and/or enhance thermal management of the engine lubricant to achieve low fuel consumption has become very little attention in the open literature. Hence, prioritizing the development of engine lubricating oil is the most essential possibility today [7-10]. In this aspect, viscosity is also an important characteristic in engine oil lubrication that is affected by temperature, shear rate and solid volume percentage, *etc*. [11]. In a moving automobile system, usually engine temperature arises to high levels and the fluid lubricant's boundary film gets collapsed, resulting in adhesion and surface damage to the sliding metallic surfaces [12,13]. Hence, the development of high-quality lubricants may able to withstand intense pressure and high temperature working conditions as well [14].

To improve the quality of lubricating oil, nanomaterials can be added to improve its tribological properties which may reduce overall frictional losses in engines, because of their

improved mechanical properties. Nanomaterials have gained immense interest in recent years due to their versatility and usability in a range of energy-related disciplines [15,16]. Metal and metal-oxide nanoparticles, layered nanomaterials and carbon-based nanomaterials are most used examples of nanomaterials having distinct properties [17,18]. Till date, the viscosity factor of engine oil lubricant has mostly studied and it was found that the viscosity of the nanofluid usually drops with increasing temperature where size of the nanoparticles may affect significantly [19]. Primarily, improving fuel efficiency by reducing friction has been one of the most serious difficulties confronting the vehicle industry [20]. Therefore, to reduce the frictional damage on metallic surfaces, a lubricating layer between the mating layers can be provided which is a very small factor, but the most essential and most ignorable part of research in the automotive industry [21]. Typically, commercial lubricants require complex preparation techniques due to the presence of basic oils and other additives [22-25].

Herein, this work studied the impact of ZnO, MWCNT, CTAB and SDS-based nanocomposites on oil lubricant under severe temperature conditions to analyze the variations in viscosity and density parameters. One of the major reasons of choosing these nanomaterials is that they are environmentally safe [26]. ZnO as base material is selected because of its several characteristic features and can be easily morphologically tuned [27,28]. Further, MWCNTs are blended with ZnO nanoparticles to make nanocomposite because CNTs are having extremely high mechanical strength, friction-less carbonaceous outer surface, high hydrophobicity, flexibility, *etc*. Because of their unique structural and mechanical properties along with the self-lubricating effect, CNTs have been employed as lubricant additives with ZnO to increase the performance of basic lubricants in terms of friction reduction, temperature dependent viscosity and density [29]. Furthermore, for comparative analysis of ZnO-based nanocomposites with surface encapsulated ZnO nanomaterials, two major surfactants such as SDS and CTAB have also used with ZnO nanoparticles, which may have some distinct factors such as (i) colloidal stability, (ii) good hydrophobicity and (iii) moderate solubility [30]. These surfactant molecules at liquid/liquid interfaces are widely recognized for the formation and stabilization of microemulsions [31].

To improve the oil lubrication performance by minimizing frictional factors and improve the engine's overall performance, the present work has mainly focused on developing one of the key factors of lubricant oil *i.e.* viscosity (kinematic as well as dynamic). For this purpose, ZnO and ZnO-based nanoadditives are added into the petrol engine lubricant 20W40 oil and studied the viscosity fluctuations. All the nanocomposites including ZnO, ZnO/MWCNT 1%, 2%, 3%, ZnO/SDS and ZnO/CTAB were synthesized by facile sol-gel process and simultaneously, investigated the viscosity behaviour of nanoparticle in petrol engine lubricant (20W40). In order to determine variations in oil viscosity, an experiment was conducted to compare the viscosity test results with both kinematic and dynamic viscosity values of a commercial base oil and a nanoadditive oil. This study represents a small advancement in the development of lubricants containing non-additives, which aim to maintain viscosity at elevated operating temperatures.

EXPERIMENTAL

Analytical grades of zinc acetate ($ZnC_4H_6O_4$) (precursor, 99.5% purity), potassium hydroxide pellets (85%), MWCNT (99.9% purity), sodium dodecylsulphate (SDS) (99%), cetyltrimethylammonium bromide (CTAB) (99%) and in-house deionized water were used for the experimental synthesis purposes. All the materials were purchased from S.D. Fine Chemicals Ltd. Throughout the process, 3 L of digital ultrasonic cleaner (LABON-100 W, 40 kHz) was used frequently for carrying out the successful experimentation of the work.

Synthesis and sample preparation method: The ZnO nanoparticles were synthesized a simple and cost-effective sol-gel process [32]. As shown in Fig. 1, 30 mL of deionized water was taken, in which 3.285 g of ZnO precursor was added and stirred for 2 h at 100 ºC followed by the addition of 20 mL of 0.5 M KOH solution in a dropwise manner. Consequently, the pH level of the complete homogeneous solution was maintained between 9 to 11 and then, kept it in refluxer at 80 ºC for 4 h. Following this, the sample was dried for 1 h at 100 ºC and calcined at 500 ºC for 3 h to get the crystalline material. The prepared sample was then collected and ground by traditional mortar-pestle technique to get fine powder and processed for further experimentation and characterizations. Similarly, for the synthesis of ZnO/MWCNT nanocomposite sample, a similar process was followed while in the second step of the solution preparation, commercial MWCNT was added as a secondary agent.

Fig. 2 represents the basic procedure for the preparation of nanoparticles blended dispersions 20W40 engine oil in a simple way [33-36]. For the preparation of the nanoparticles dispersed oil mixture, as-synthesized ZnO NPs and ZnO/MWCNT nanocomposite samples were blended into 50 mL of as-specified lubricating oil with varying amounts of 50 mg, 100 mg and 150 mg sequentially and kept in ultrasonication for 2 h after 10 min of magnetically stirring, for equal material dispersion and distribution. A similar process was followed for the ZnO/MWCNT nanocomposite sample with different MWCNT percentages (1, 2 and 3 %). In case of ZnO-with surfactants (SDS and CTAB) based dispersion preparation, first as-synthesized ZnO nanoparticles were blended with the specified engine oil and magnetically stirred for 10 min. Then, the surfactants (CTAB and SDS) were added in two separate ZnO blended solutions and kept for ultrasonication for 2 h, respectively and named as ZnO/SDS and ZnO/CTAB.

Characterization: The characterization of synthesized nanomaterials was done by the X-ray diffraction (XRD) (Rigaku Ultima IV), Fourier-transform infrared spectroscopy (FTIR) by Perkin-Elmer Spectrum 2, scanning electrode microscopy (SEM) was carried out by Hitachi SUI510 and UV-visible spectroscopy was done by using Parkin-Elmar LAMDA 750.

The redwood viscometer was used to analyze the viscosity of the nanofluids. The cylinder consist of an inner diameter of 46.5 mm and a depth of 96 mm. The orifice has a bore of 1.62 mm and a length of 12 mm. The temperature of oil bath and

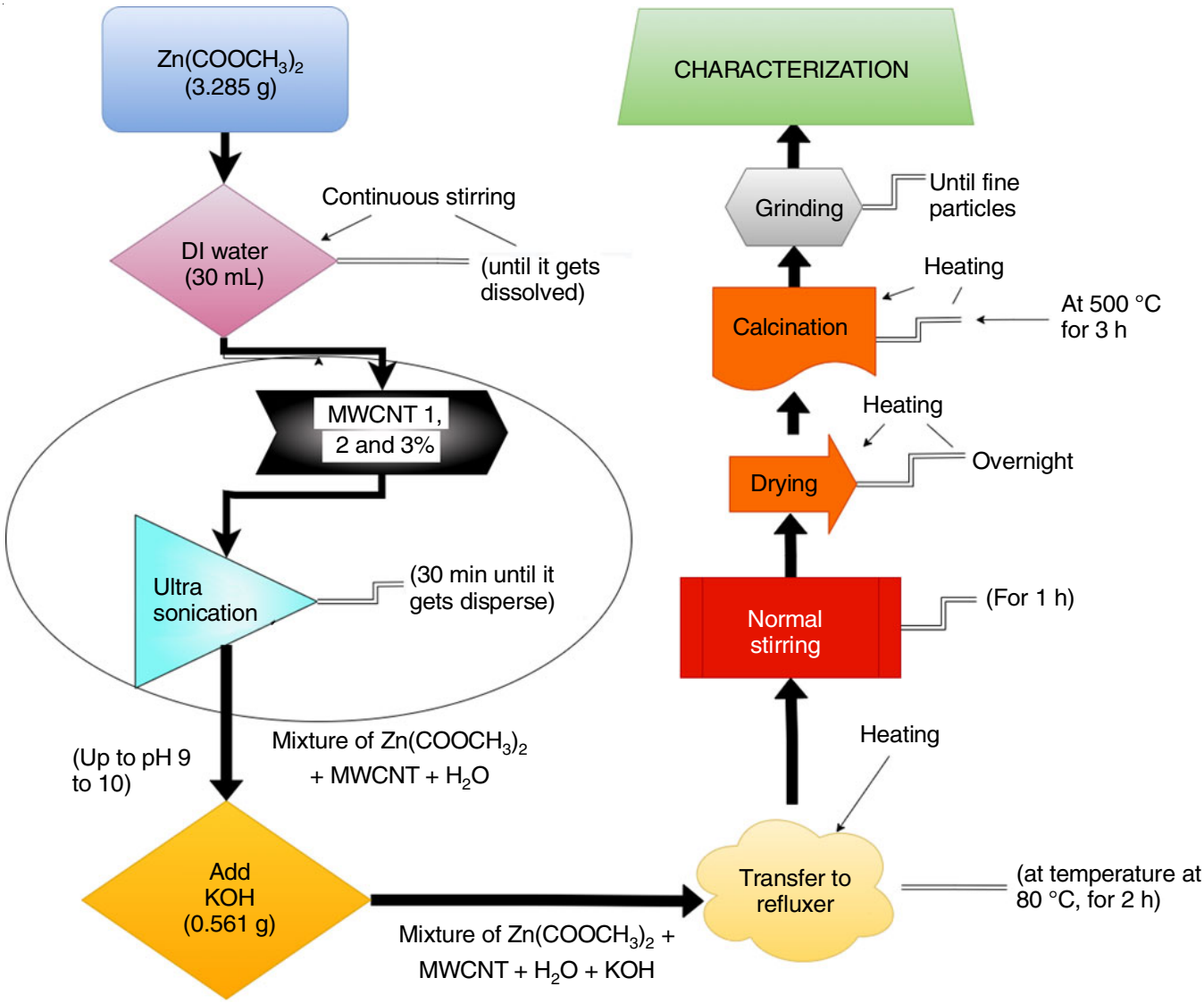

Fig. 1. Process flow chart for the synthesis of ZnO NPs and ZnO/MWCNT nanocomposite

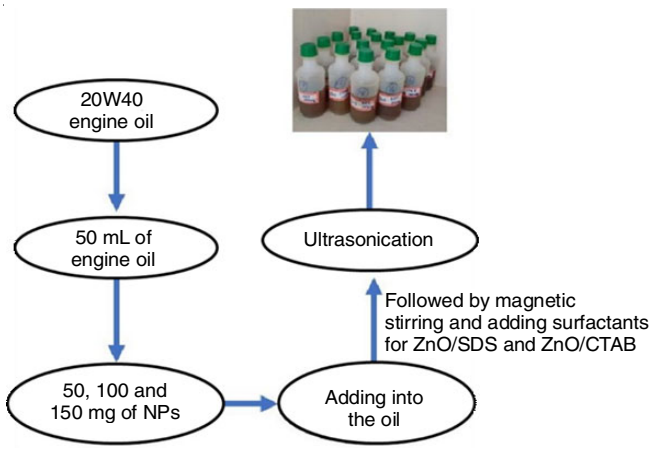

Fig. 2. Dispersing method of ZnO, ZnO/MWCNT (1, 2 and 3%), ZnO/CTAB and ZnO/SDS-based petrol engine lubricant

the temperature of water bath were controlled using two thermometers. With the jet closed, 50 mL of 20W40 oil was poured into the redwood orifice and the outer cylinder was filled with water. The receiving flask was set under its capillary tube. The stopwatch started parallel with the opening of jet by lifting the ball blocker from its spot. The water was electrically heated at various temperatures and when the water temperature reached the desired level, power was turned off and stirred the water, which used to heat up the inner cylinder tube.Once the desired temperature of the inner cylinder was reached, the duration needed to collect 30 mL of oil was recorded by opening the jet. The same procedure was followed for 20W40 lubricating oil mixed with 50 mg, 100 mg and 150 mg of ZnO nanoparticles, ZnO/MWCNT composite (1, 2 and 3%) and ZnO/surfactants (CTAB and SDS) samples. The observed readings were then used to evaluate the kinematic viscosity (in stokes) and absolute or coefficient of dynamics viscosity (in poise).

Density of the lubricant dispersions were calculated by using following empirical equation [37]:

$$\rho_T = \rho_R - 0.00065\ (T - T_R) \quad (1)$$

where ρ_T and ρ_R are the density of lubricant at experimental (T) and room temperatures (T_R), respectively.

RESULTS AND DISCUSSION

XRD studies: The XRD patterns of ZnO NPs synthesized by the sol-gel method are shown in Fig. 3. All the diffraction peaks in the XRD pattern confirmed the hexagonal crystal structure with the standard JCPDS card no. 36-1451 [38]. The XRD pattern also demonstrates the excellent purity of the product with single phase crystalline structure. Further calcination at high temperature, synthesized ZnO NPs formed with high crystallinity. Calcination at high temperatures causes grain size to move, causing small grains to combine and produce larger grains. Similarly, the XRD patterns of ZnO and ZnO/MWCNT (1 and 3%) are shown in Fig. 3. The incorporation of CNTs in the structure of ZnO did not affect much the structural patterns of ZnO. With the increasing percentage of CNTs in the ZnO/MWCNT nanocomposite, the crystalline diffraction peaks intensities are slightly reduced which may attribute to the poor crystallinity of CNTs and the nanoparticles were connected to the hexagonal phase of graphite and graphitic planes. The diffraction peaks at 2θ = 31.84º, 34.49º, 36.33º, 47.63º, 56.65º, 62.92º, 66.44º, 68.00º, 69.15º, 72.63ºº and 77.03º are assigned to the *hkl* diffraction planes of (100), (002), (101), (102), (110), (103), (200), (112), (201), (004) and (202), respectively.

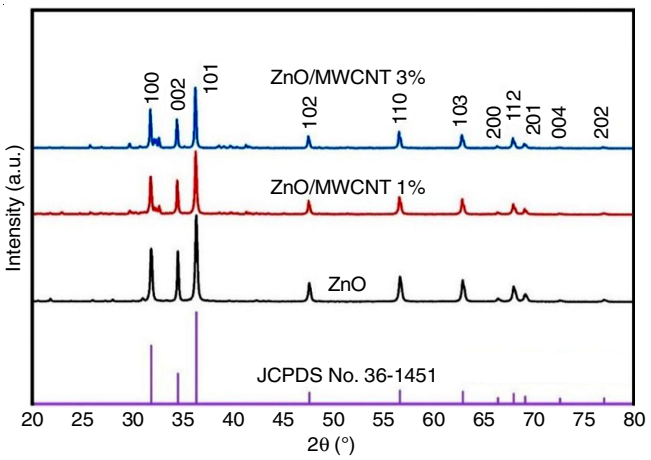

Fig. 3. XRD pattern of ZnO, ZnO/MWCNT nanocomposites with 1 and 3% of MWCNT

SEM studies: The morphological SEM views of the as-synthesized ZnO nanoparticles and ZnO/MWCNT (1 and 3%) are shown in Fig. 4a-c. The SEM image showed that ZnO nanoparticles have almost spherical shape with highly susceptible to aggregation by packing of nanoparticle aggregates, confirmed that the ZnO nanoparticles tended to accumulate and did not allow the identification of a single particle due to the high surface energy at nanosize [39,40]. The larger particles shown in the SEM image are the result of high aggregation. As shown in Fig. 4b-c, the ZnO/MWCNT (with 1 and 3%) nanocomposite samples, hardly the clear view of CNTs is visible due to low content of the nanotubes and narrow diameter. Further for the compositional confirmation, EDX spectra of the samples were also measured. As shown in Table-1, the elemental percentages in synthesized ZnO/MWCNT 1 and 3% were found out and higher carbon content in 3% MWCNT composite was due to the higher percentage of CNT in the composite sample. Thus, all the elements observed in the EDX observation were the evidence of MWCNT presence with ZnO NPs, which are also illustrated by Fig. 5.

TABLE-1
EDX ANALYSIS FOR IDENTIFYING THE ELEMENTAL COMPOSITION OF THE SYNTHESIZED SAMPLES

Sample	Atomic (wt.%)		
	C	O	Zn
ZnO	–	31.8	68.2
ZnO/MWCNT 1%	41.8	17.3	40.9
ZnO/MWCNT 3%	71.6	16.7	11.7

FTIR studies: Fig. 6 shows the FTIR spectra of the pure ZnO and all ZnO-based materials [41]. The presence of IR peaks can be detected in the material which correlated to the presence of standard carboxylate and hydroxyl impurities in the materials. More particularly, the broad band at 3195 cm^{-1} was attributed to the hydroxyl groups of O-H stretching mode. The spectrum at fingerprint region, the traces of carboxylate impurities disappeared, indicating a possibility of zinc carboxylate breakdown and conversion to ZnO during the calcination process [42,43]. The ZnO/MWCNT- 1, 2 and 3% showed C=C vibration band at 1566 cm^{-1} which originated due to the incorporation of CNT. The ZnO/SDS composites transmittance peaks at 1484 cm^{-1} and 1344 cm^{-1} assigned as C-H and C-N stretching. For ZnO/CTAB transmittance peaks at 1572 cm^{-1} can be assigned to the C-C stretching, 1481 cm^{-1} for C-H and 1350 cm^{-1} for C-N stretching. For all the samples in the FTIR study, presence of O-H group has been observed attributing to the absorption of atmospheric moisture and the peak at 523 cm^{-1} corresponds to hexagonal ZnO (Raman active).

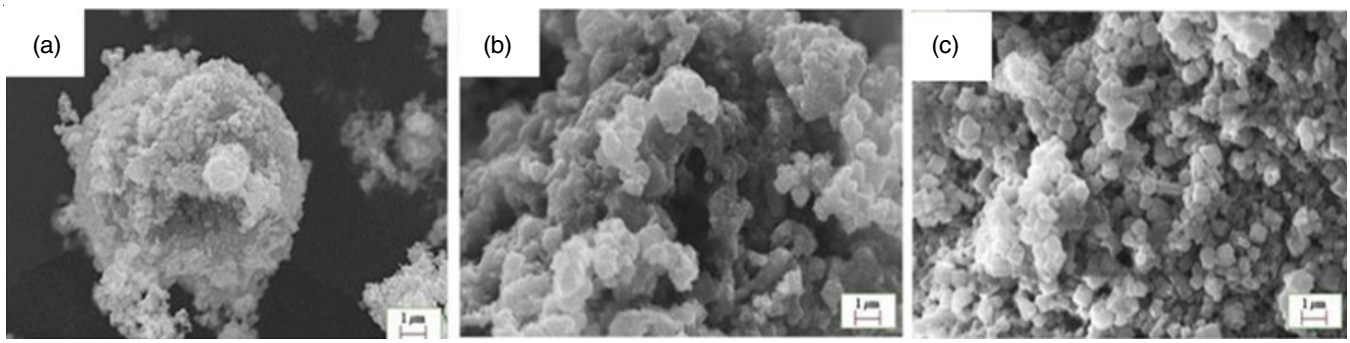

Fig. 4. SEM images of (a) ZnO, (b) ZnO/MWCNT 1% and (c) ZnO/MWCNT 3% nanoparticles

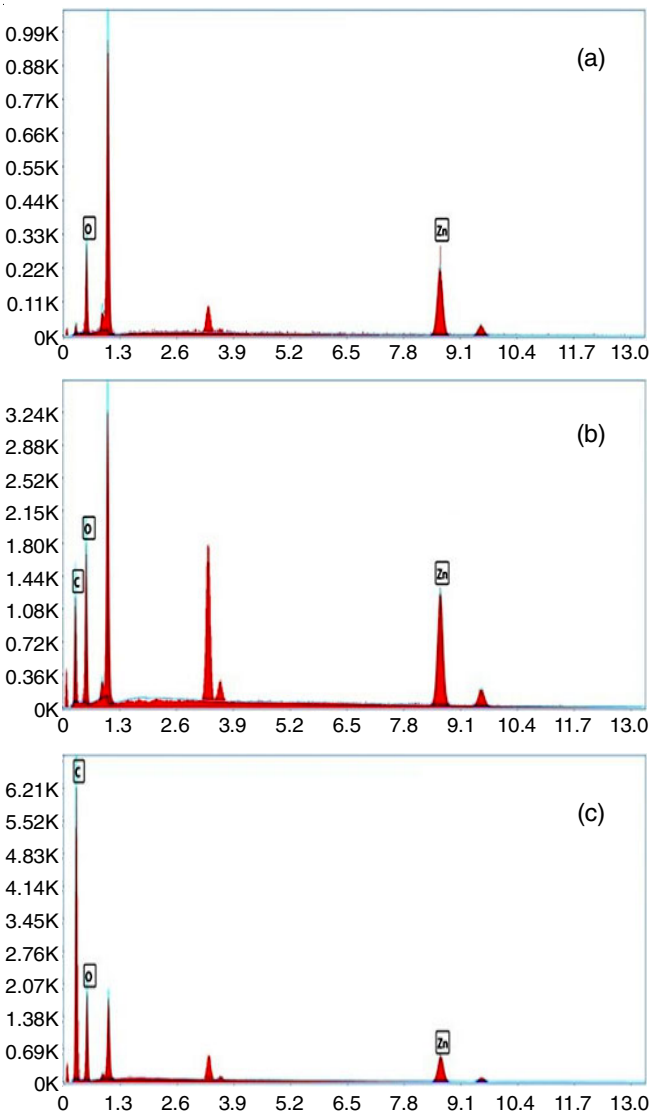

Fig. 5. EDX analysis of (a) ZnO, (b) ZnO/MWCNT 1% and (c) ZnO/MWCNT 3% nanoparticles

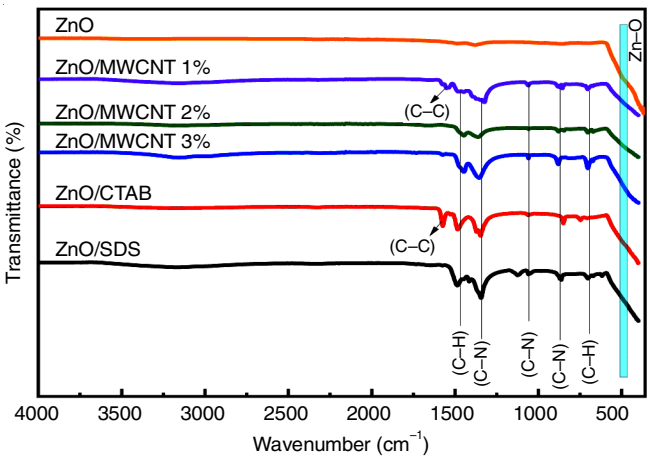

Fig. 6. FTIR spectral results of the synthesized samples of pure-ZnO, ZnO/MWCNT composite (for 1, 2 and 3%), ZnO/CTAB and ZnO/SDS

UV-visible studies: Fig. 7 shows the UV-visible absorption spectra of all the synthesized samples. Based on the spectra, the concentration, absorptivity and absorption wavelength of the

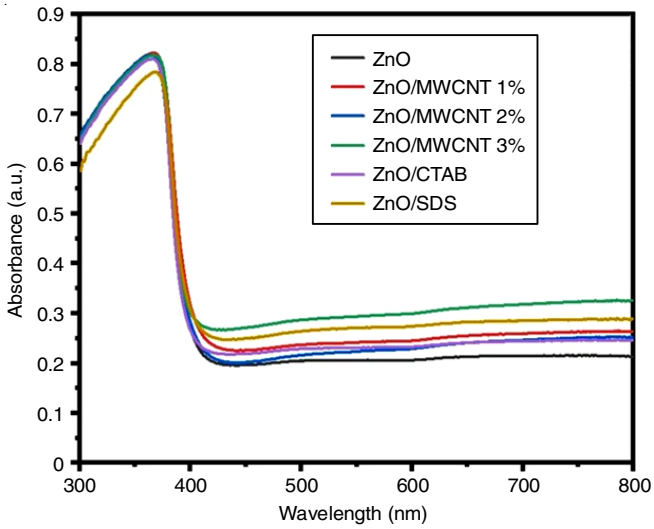

Fig. 7. UV-visible absorption spectra of the synthesized pure-ZnO, ZnO/MWCNT (1, 2 and 3%), ZnO/CTAB and ZnO/SDS

synthesized ZnO NPs and ZnO-based composite and capped samples are confirmed. The activation region of the samples in UV length is responsible for the highest absorbance at 350 nm, which is the standard absorbance value for ZnO and confirms its existence in all samples. Further, the incorporation of CNT slightly enhanced the absorbance of the samples as shown in Fig. 7. There was no noticeable difference between dark current and photocurrent when focused with a visible light of wavelength of 400-700 nm on the homojunction. The result got changed when UV light (λ = 325 nm) was exposed [44].

Viscosity studies: All the tested lubricant viscosities were determined and plotted as a function of temperature. A change in temperature will cause a change density and *vice-versa* also [45]. The density of the oil blends was reduced as an increase in the temperature (Table-2). At 34 ºC, it was observed that the density of base oil was 0.866 g/cc, at 44 ºC 0.860 and at 54 ºC 0.853 g/cc for base oil and similarly for blended oil with nanomaterials (ZnO, ZnO/MWCNT 1, 2 and 3%, ZnO/SDS and ZnO/CTAB) are shown in Table-2.

The viscosity of a fluid is a property that comes from collisions between neighboring particles moving at different speeds. When fluid flows through an opening channel, the molecules of the fluid normally move more quickly toward the opening center and more slowly toward its wall. It was revealed that at low temperature, both 20W40 and nano-oils behave like Newtonian fluids in terms of viscosity and it may be attributed to the presence of ZnO nanoparticles causing the increase in lubricant viscosity. Fig. 8 represents the kinematic and dynamic viscosity graph of 20W40 lubricating oil. With the change in temperature of base oil, both the kinematic and the dynamic viscosity reduced such as the kinematic viscosities were 1.88, 0.75 and 0.54 stokes at 34, 44 and 54 ºC and the dynamic viscosities were 1.63, 0.65 and 0.46 poise at 34, 44 and 54 ºC, respectively.

Fig. 9 shows the effect of ZnO NPs concentration (50, 100 and 150 mg) on the kinematic and dynamic viscosities at different temperatures of 34, 44 and 54 ºC, respectively. The

TABLE-2
THE DENSITY (ρ_T) PARAMETERS OF 15W40 OIL BLENDED WITH ZnO, ZnO/MWCNT 1, 2 AND 3%, ZnO/CTAB AND ZnO/SDS SAMPLES WITH CARRYING TEMPERATURE

Materials	Density (g/cc)	Temperature (°C)
ZnO	0.86667	34
	0.86027	44
	0.85387	54
ZnO/MWCNT-1%	0.86666	34
	0.86026	44
	0.85386	54
ZnO/MWCNT-2%	0.86666	34
	0.86026	44
	0.85386	54
ZnO/MWCNT-3%	0.86666	34
	0.86026	44
	0.85386	54
ZnO/SDS	0.86666	34
	0.86026	44
	0.85386	54
ZnO/CTAB	0.86666	34
	0.86026	44
	0.85386	54

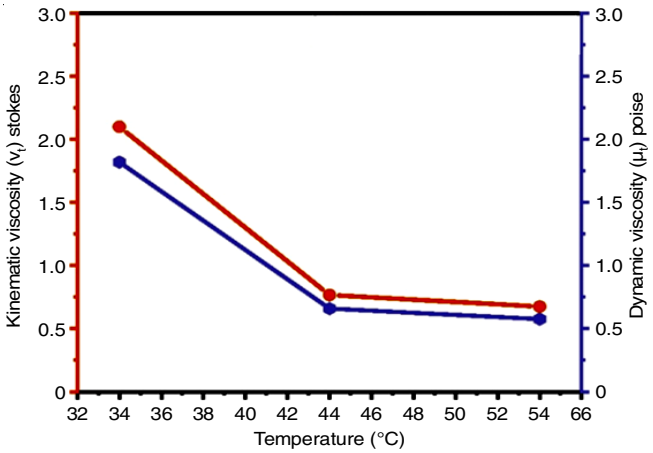

Fig. 8. Kinematic viscosity and dynamic viscosity *vs*. temperature graph of base 20W40 oil

kinematic viscosity and dynamic viscosity of ZnO NPs blended oil has increased while compared to the base 20W40 petrol engine oil. Also, it was found that 100 mg ZnO added sample showed higher kinematic and dynamic viscosities of 2.398 stokes and 2.078 poise at 34 ºC, respectively. For 50 mg added, sample showed lower kinematic and dynamic viscosities of 0.544 stokes and 0.464 poise at 54 ºC. The presence of ZnO NPs in the oil layers may be attributed to the increase in the oil viscosity.

Fig. 10 shows the effect of temperature on the kinematic and dynamic viscosities for ZnO/MWCNT composite blended oil samples. The kinematic and dynamic viscosities of 20W40 oil with ZnO/MWCNT 1% were determined at 34 ºC and increased temperatures of 44 and 54 ºC with the material dosage amounts of 50, 100 and 150 mg. Dynamic viscosity *vs*. temperature graph showed that the ZnO/MWCNT 1% of 100 mg blended dispersion sample showed the viscosity value of 1.98 poise at 34 ºC and kinematic viscosity showed that the ZnO/MWCNT 1 and 2% of 100 and 150 mg both have higher viscosity values of 2.2866 and 2.28 stokes at 34 ºC, respectively which much higher than the base oil attributing to the addition of ZnO/MWCNT composite in the oil mixture [46-50]. When compared to the base oil kinematic viscosity, the kinematic viscosity of MWCNT (2% and 1%, 150 mg and 100 mg, respectively) mixed oil was increased to 0.405 stokes, because the high thermal conductivity of the MWCNT may help in increase the viscosity of oil [51].

Fig. 11 depicts the effect of temperature on the kinematic and dynamic viscosities of ZnO/SDS added oil sample. The kinematic viscosity of the 20W40 oil with ZnO/SDS was evaluated at 34, 44 and 54 ºC, with the dosage amounts of 50,100 and 150 mg, respectively. It was observed that the kinematic viscosity of the oil sample (for 50 mg added sample) was increased to 1.9309 stokes and the dynamic viscosity was increased to 1.67346 poise at 34 ºC, while the kinematic viscosity of base oil at 34 ºC was 1.8814 stokes. Compared to the base oil kinematic viscosity, ZnO/SDS added sample showed 0.0495

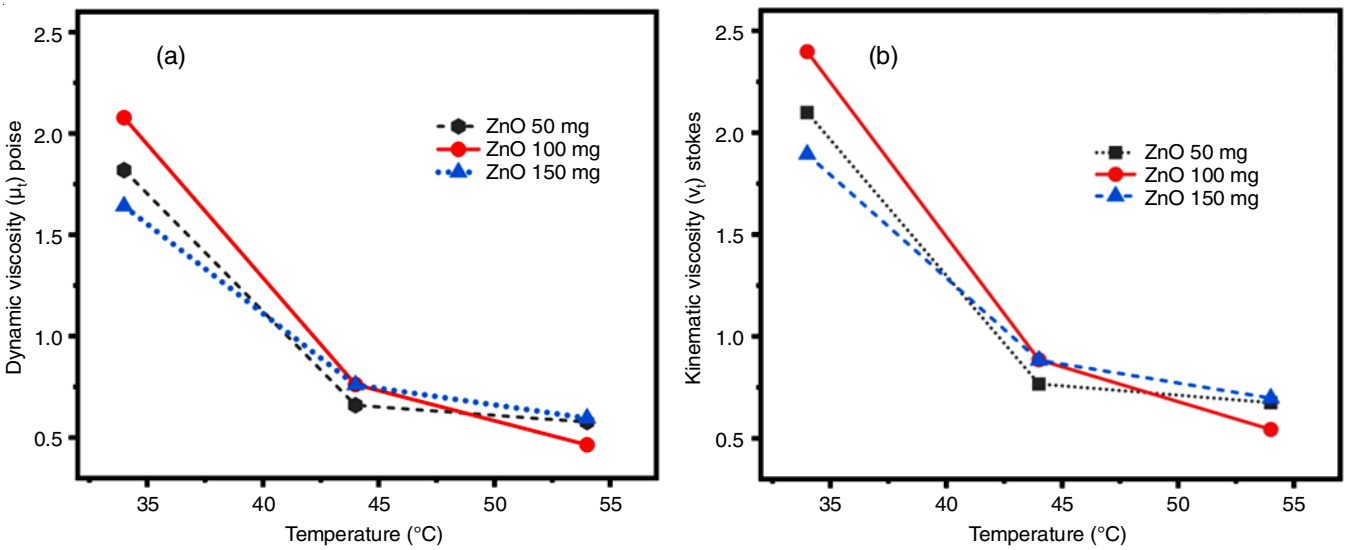

Fig. 9. Kinematic and dynamic viscosity of pure-ZnO NPs blended engine oil with different blending amount (a) kinematic viscosity and (b) dynamic viscosity

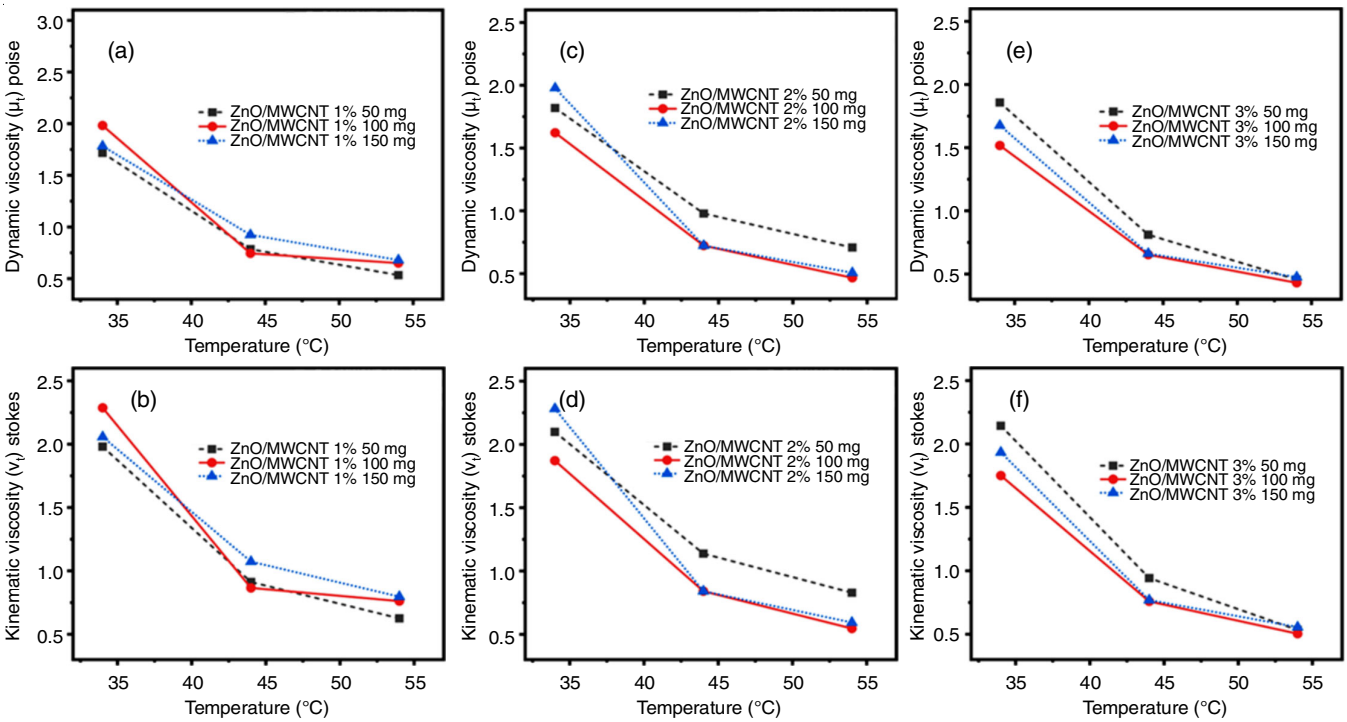

Fig. 10. Viscosity measurements of ZnO/MWCNT nanocomposites including 1, 2 and 3% blended engine oil with the varying dosage amounts of 50, 100 and 150 mg (a) dynamic viscosity of 1% MWCNT added sample, (b) kinematic viscosity 1% MWCNT added sample, (c) dynamic viscosity of 2% MWCNT added sample, (d) kinematic viscosity 2% MWCNT added sample, (e) dynamic viscosity of 3% MWCNT added sample and (f) kinematic viscosity of 3% MWCNT added oil sample

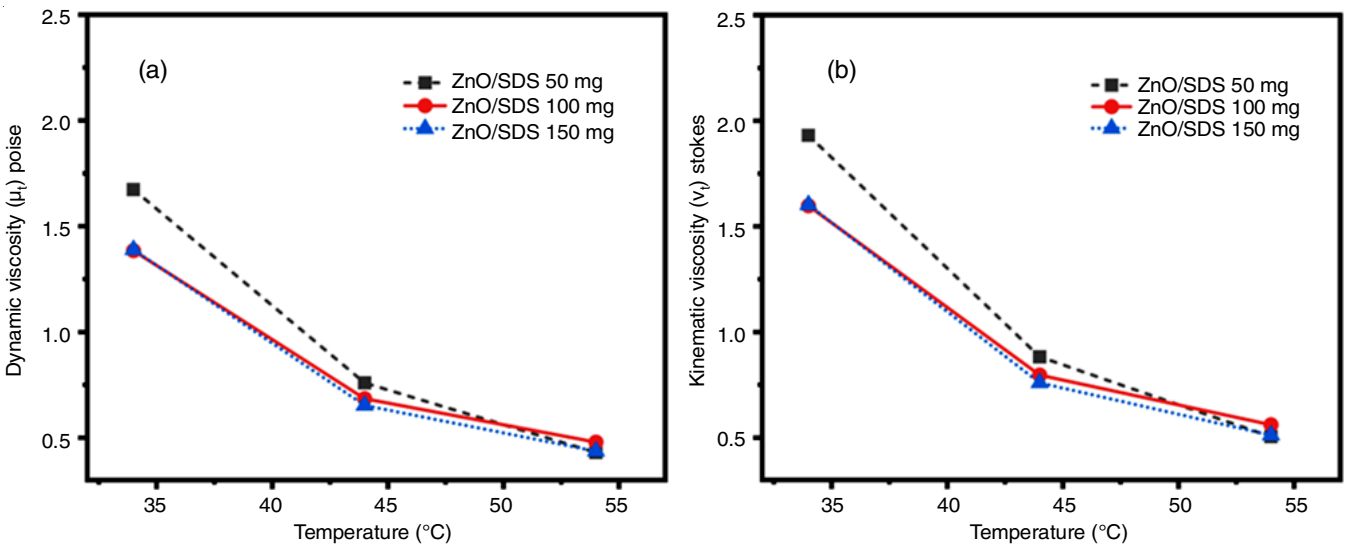

Fig. 11. Viscosity graph of ZnO/SDS added oil samples with the dosage amounts of 50, 100 and 150 mg showing dynamic and kinematic viscosity *vs*. temperature

stokes of higher kinematic viscosity, which may attribute to the formation of enhanced and stable oil dispersion in the presence of SDS.

In addition to the nanocomposite added engine oil sample, SDS and CTAB were added to the ZnO blended oil mixtures in order to modify the surface property and develop a well-dispersed oil colloidal solution [52]. The ZnO and CTAB were employed to study the change in lubricating oil kinematic and dynamic viscosity with varying temperatures and dosage amounts as shown in Fig. 12. The dynamic viscosity of lubricating oil with ZnO/CTAB (150 mg) reached 1.9154 poise at 34 ºC and the kinematic viscosity reached (dosage of 150 mg) to 2.210 stokes at 34 ºC. Compared to the base oil dynamic viscosity, the ZnO/CTAB has 0.284 poise higher viscosity and kinematic viscosity of 0.329 stokes increased at 34 ºC.

Fig. 13a-b compares the kinematic and dynamic viscosities of all higher values of suspended nanoparticles blended engine oil based colloidal mixture. The kinematic and dynamic viscosities of ZnO NPs blended lubricant (100 mg dosage) at 34 ºC were 2.09891 strokes and 2.078 poise, which are the highest

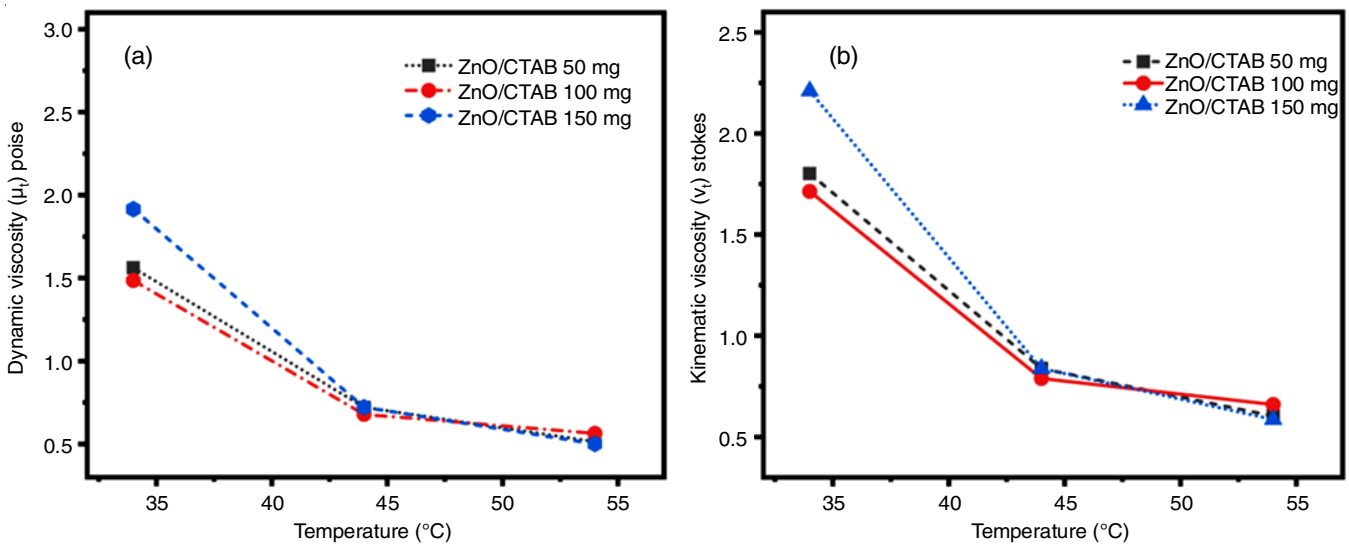

Fig. 12. Viscosity graph of ZnO/CTAB nanoparticle of 50, 100 and 150 mg (a) kinematic viscosity *vs*. temperature (b) dynamic viscosity *vs*. temperature

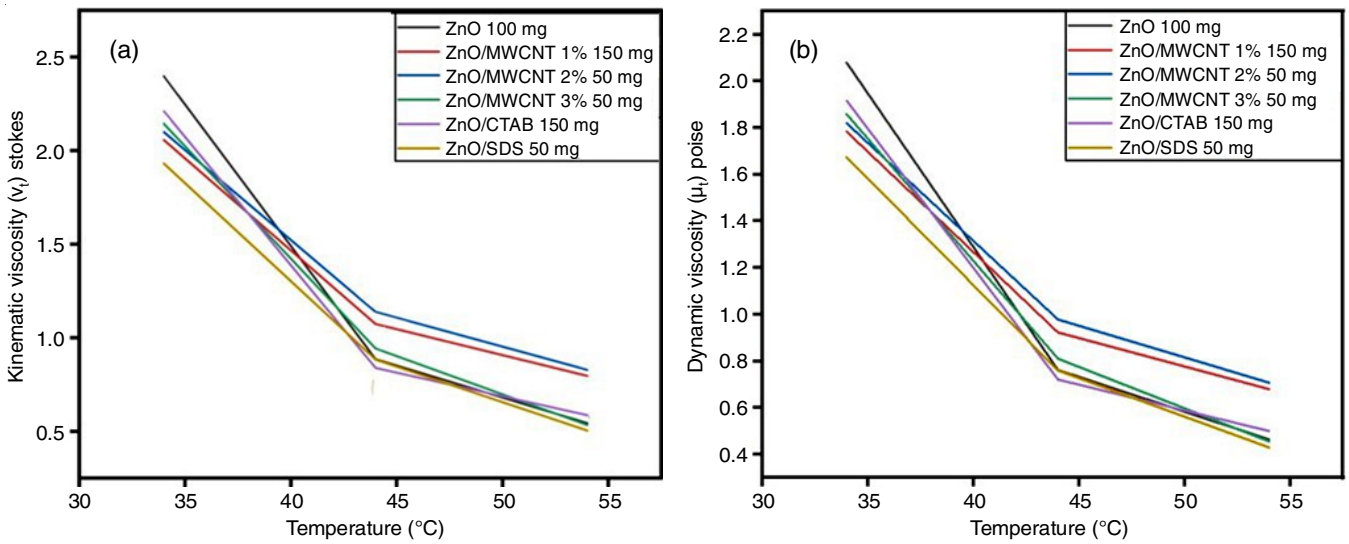

Fig. 13. Viscosity graph of higher viscosity of different nanoparticles with different concentration (a) kinematic viscosity *vs*. temperature (b) dynamic viscosity *vs*. temperature

values among the nano-lubricant's kinematic and dynamic viscosity readings. When the temperature increased to 44 and 54 ºC, the kinematic viscosity of ZnO/MWCNT 2% (50 mg) climbs to 1.1375 and 0.82843 strokes, which is comparatively higher than that of other nano-lubricants. In comparison to all nano-lubricants, ZnO/SDS depicted the lowest viscosity index at 34 and 54 ºC, respectively.

Further, the stability of the as-prepared colloidal engine oil dispersions was also observed visually as well as spectral measurement for up to 12 days as shown in Fig. 14a-e. As observed in the visual photographs, the dispersion stability may not be clear that much, but from the UV-spectra measurements, it can be concluded that the highest stability was shown by ZnO/CTAB blends due to their well-surfaced encapsulation of ZnO NPs and, in comparison to ZnO/MWCNT 2% absorbs the second good stability.

Conclusion

ZnO nanoparticles and their composites with MWCNT, sodium dodecyl sulfate (SDS) and cetyltrimethylammonium bromide (CTAB) as surfactant/capping agents were synthesized successfully using a facile sol-gel approach. The corresponding measurements were carried out using different characterization techniques and identified the structural and morphological features. The XRD pattern of as-synthesized ZnO nanoparticles was well-fitted with the ZnO crystal structure of stable wurtzite phase. ZnO nanoparticles and its corresponding nanocomposite with MWCNT and blends with CTAB and SDS were mixed in petrol engine lubricating oil of 20W40 grade simultaneously to analyze the respective viscosity performance as well as colloidal stability. The viscosity test was carried out at different temperatures of 34, 44 and 54 ºC for each dosage of 50, 100 and150 mg in oil. The variations in kinematic viscosities

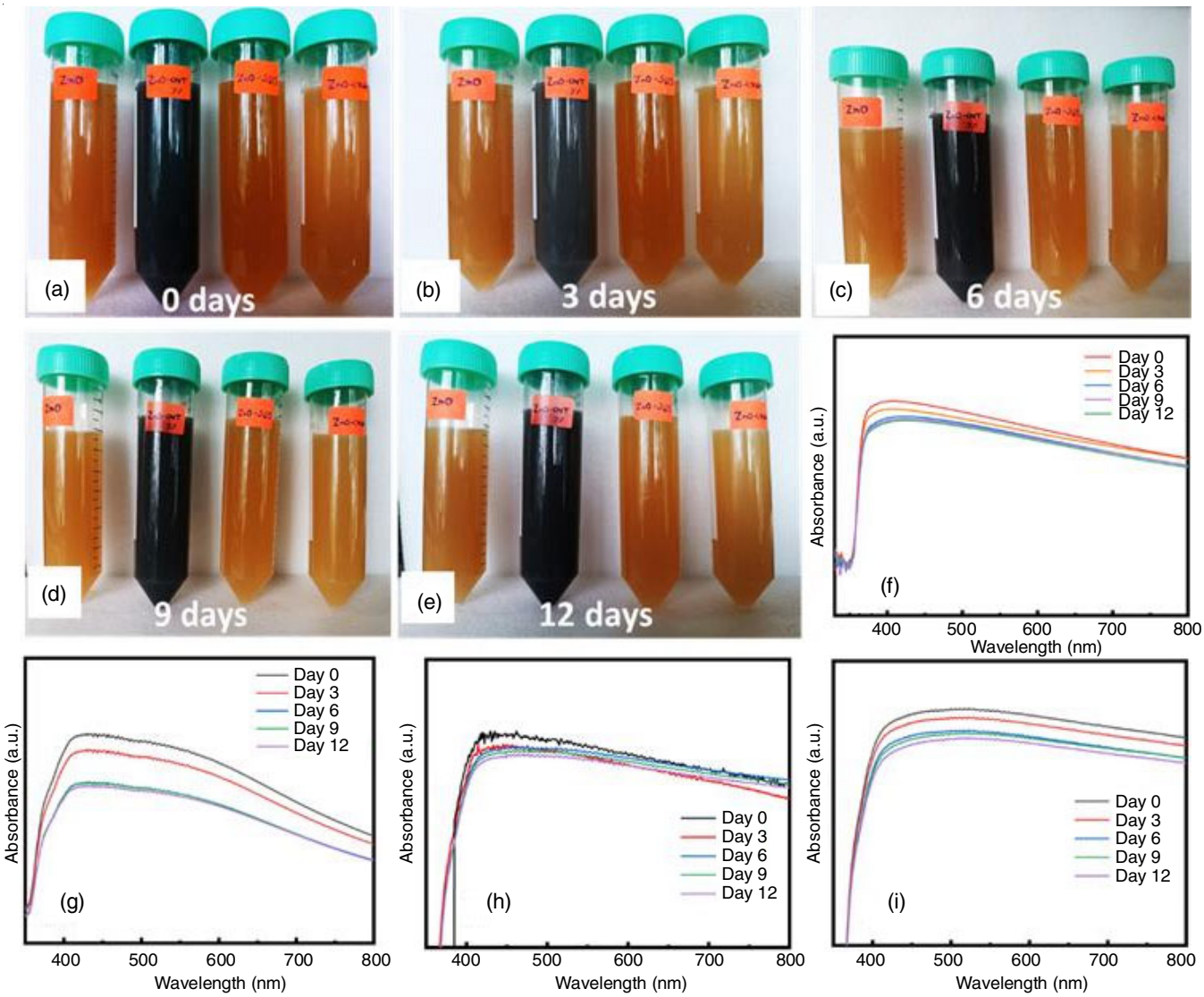

Fig. 14. (a-e) Photographs of dispersion stability of the nanomaterials blended colloidal engine oil mixture; and UV-assisted stability measurement for (f) pure ZnO added oil, (g) ZnO/MWCNT added oil, (h) ZnO/CTAB added oil and (i) ZnO/SDS added oil samples

were observed with gradual increase in temperature of lubricant and the viscosity was reduced accordingly. This viscosity reduction phenomena were observed in both normal base oil and nanoparticle dispersed oil in a parallel trend. The optimum viscosity performance was observed at 54 ºC for the ZnO/MWCNT 2% 100 mg, ZnO/SDS 50 mg and ZnO/CTAB 150 mg samples. Thus, the present study can be taken forward further to improve the wear properties, cooling rate and fuel efficiency by adding potential novelty in materials properties and intrinsic physico-chemical characteristics to overcome the oil consumption and further improvement of the overall engine performance.

ACKNOWLEDGEMENTS

The authors thank the Department of Applied Sciences (Nanotechnology), Visvesvaraya Technological University, Muddenahalli, India for providing research and characterization facilities. The authors also thank Department of Aeronautical and Automobile Engineering, Manipal Institute of Technology (MAHE), Manipal, India for supporting to carry out the research experimental works under the project.

CONFLICT OF INTEREST

The authors declare that there is no conflict of interests regarding the publication of this article.

REFERENCES

1. M. Ross, *Contemp. Phys.*, **38**, 381 (1997); https://doi.org/10.1080/0010751971821 99
2. J.-S. Chen and H.-Y. Hwang, *Proc. Inst. Mechan. Eng. Part D: J. Automob. Eng.*, **227**, 1303 (2013); https://doi.org/10.1177/0954407013491184
3. G.T. Kalghatgi, *Proc. Combust. Inst.*, **35**, 101 (2015); https://doi.org/10.1016/j.proci.2014.10.002
4. G. Antoni, *The Scientific World J.*, **2014**, 523281 (2014); https://doi.org/10.1155/2014/523281
5. A. Baumann and B. Bertsche, *Forsch Ingenieurwes*, **86**, 795 (2022); https://doi.org/10.1007/s10010-022-00589-9

6. Z. Rasep, M.N.A.W.M. Yazid and S. Samion, *Renew. Sustain. Energy Rev.*, **146**, 111191 (2021); https://doi.org/10.1016/j.rser.2021.111191
7. H. Pourpasha, S.Z. Heris and Y. Mohammadfam, *Sci. Rep.*, **11**, 11064 (2021); https://doi.org/10.1038/s41598-021-90625-5
8. J.G. Hawley, C.D. Bannister, C.J. Brace, S. Akehurst, I. Pegg and M.R. Avery, *Proc. Inst. Mechan. Eng. Part D: J. Automob. Eng.*, **224**, 1213 (2010); https://doi.org/10.1243/09544070JAUTO1534
9. D. Wu, *IOP Conf. Ser.: Mater. Sci. Eng*., **493**, 012008 (2019); https://doi.org/10.1088/1757-899X/493/1/012008
10. K. Cheenkachorn and B. Fungtammasan, *Energy*, **35**, 2552 (2010); https://doi.org/10.1016/j.energy.2010.03.002
11. M. Afrand, K. Nazari Najafabadi and M. Akbari, *Appl. Therm. Eng.*, **102**, 45 (2016); https://doi.org/10.1016/j.applthermaleng.2016.04.002
12. A. Hernandez-Battez, J.E. Fernandez-Rico, A. Navas-Arias, J.L. Viesca Rodriguez, R. Chou-Rodriguez and J.M. Diaz-Fernandez, *Wear*, **261**, 256 (2006); https://doi.org/10.1016/j.wear.2005.10.001
13. Y. Wang, T. Ren and J. Li, Tribological Studies on a Novel Borate Ester containing Benzothiazol-2-yl and Disulfide Groups as EP and Multifunctional Additive, In: Advanced Tribology, Springer Berlin Heidelberg, Berlin, Heidelberg, pp. 894–895 (2009).
14. S. Sarkar and R. Sarkar, *Mater. Today Proc.*, **44**, 3606 (2021); https://doi.org/10.1016/j.matpr.2020.09.595
15. M. Gulzar, H.H. Masjuki, M.A. Kalam, M. Varman, N.W.M. Zulkifli, R.A. Mufti and R. Zahid, *J. Nanopart. Res.*, **18**, 223 (2016); https://doi.org/10.1007/s11051-016-3537-4
16. M. Asrul, N.W.M. Zulkifli, H.H. Masjuki and M.A. Kalam, *Procedia Eng.*, **68**, 320 (2013); https://doi.org/10.1016/j.proeng.2013.12.186
17. M.M. Rahman, M. Islam, R. Roy, H. Younis, M. AlNahyan and H. Younes, *Lubricants*, **10**, 281 (2022); https://doi.org/10.3390/lubricants10110281
18. S. Mobasser, A.A. Firoozi, *J. Civil Eng. Urbanism*, **6**, 84 (2016).
19. A.A. Nadooshan, M.H. Esfe and M. Afrand, *Physica E*, **92**, 47 (2017); https://doi.org/10.1016/j.physe.2017.05.011
20. C.M. Taylor, *Wear*, **221**, 1 (1998); https://doi.org/10.1016/S0043-1648(98)00253-1
21. R. Tonk, *Mater. Today Proc.*, **37**, 3475 (2021); https://doi.org/10.1016/j.matpr.2020.09.384
22. J. Wang, W. Zhuang, W. Liang, T. Yan, T. Li, L. Zhang and S. Li, *Friction*, **10**, 645 (2022); https://doi.org/10.1007/s40544-021-0511-7
23. R.M. Mortier, M.F. Fox and S. Orszulik, Chemistry and Technology of Lubricants, Springer, edn. 3 (2010).
24. R.R. Leslie, Lubricant Additives, Chemistry and Applications, Marcel Dekker, Inc., pp. 293-254 (2003).
25. S.Q.A. Rizvi, A Comprehensive Review of Lubricant Chemistry, Technology, Selection and Design, ASTM International, West Conshohocken, PA., pp. 100-112 (2009).
26. Y.J.J. Jason, H.G. How, Y.H. Teoh and H.G. Chuah, *Processes*, **8**, 1372 (2020); https://doi.org/10.3390/pr8111372
27. B. Ren, L. Gao, B. Xie, M. Li, S. Zhang, G. Zu and X. Ran, *Tribol. Int*., **144**, 106114 (2020); https://doi.org/10.1016/j.triboint.2019.106114
28. A.C. Janaki, E. Sailatha and S. Gunasekaran, *Spectrochim. Acta A Mol. Biomol. Spectrosc.*, **144**, 17 (2015); https://doi.org/10.1016/j.saa.2015.02.041
29. B.S.A. Vardhaman, M. Amarnath, J. Ramkumar and K. Mondal, *Mater. Chem. Phys.*, **253**, 123447 (2020); https://doi.org/10.1016/j.matchemphys.2020.123447
30. A.Q. Shen, B. Gleason, G.H. McKinley and H.A. Stone, *Phys. Fluids*, **14**, 4055 (2002); https://doi.org/10.1063/1.1512287
31. Y. Li, Y. Guo, M. Bao and X. Gao, *J. Colloid Interface Sci.*, **361**, 573 (2011); https://doi.org/10.1016/j.jcis.2011.05.078
32. M. Parashar, V.K. Shukla and R. Singh, *J. Mater. Sci. Mater. Electron.*, **31**, 3729 (2020); https://doi.org/10.1007/s10854-020-02994-8
33. N. Desai, A.M. Nagaraj and N. Sabnis, *Mater. Today Proc.*, **47**, 5646 (2021); https://doi.org/10.1016/j.matpr.2021.03.688
34. A. Amiri, M. Shanbedi, H. Amiri, S.Z. Heris, S.N. Kazi, B.T. Chew and H. Eshghi, *Appl. Therm. Eng.*, **71**, 450 (2014); https://doi.org/10.1016/j.applthermaleng.2014.06.064
35. M. Shanbedi, S.Z. Heris, A. Amiri and H. Eshghi, *J. Taiwan Inst. Chem. Eng.*, **60**, 547 (2016); https://doi.org/10.1016/j.jtice.2015.10.008
36. M. Shanbedi, S.Z. Heris and A. Maskooki, *J. Therm. Anal. Calorim.*, **120**, 1193 (2015); https://doi.org/10.1007/s10973-015-4404-8
37. M. Zolfalizadeh, S.Z. Heris, H. Pourpasha, M. Mohammadpourfard and J.P. Meyer, *Int. J. Energy Res.*, **2023**, 3477673 (2023); https://doi.org/10.1155/2023/3477673
38. P. Basnet, D. Samanta, T.I. Chanu, J. Mukherjee and S. Chatterjee, *SN Appl. Sci.*, **1**, 633 (2019); https://doi.org/10.1007/s42452-019-0642-x
39. I. Stanciu, *Seria Chimie*, **23**, 27 (2012).
40. R. Hong, T. Pan, J. Qian and H. Li, *Chem. Eng. J.*, **119**, 71 (2006); https://doi.org/10.1016/j.cej.2006.03.003
41. Y.W. Lai, E.K. Kemsley and R.H. Wilson, *Food Chem.*, **53**, 95 (1995); https://doi.org/10.1016/0308-8146(95)95793-6
42. A.K. Zak, W.H.A. Majid, M. Darroudi and R. Yousefi, *Mater. Lett.*, **65**, 70 (2011); https://doi.org/10.1016/j.matlet.2010.09.029
43. K. Holmberg, P. Andersson and A. Erdemir, *Tribol. Int.*, **47**, 221 (2012); https://doi.org/10.1016/j.triboint.2011.11.022
44. P. Gago-Ferrero, M.S. Díaz-Cruz and D. Barceló, *Anal. Bioanal. Chem.*, **404**, 2597 (2012); https://doi.org/10.1007/s00216-012-6067-7
45. F. Noel, *Thermochim. Acta*, **4**, 377 (1972); https://doi.org/10.1016/0040-6031(72)87019-9
46. A. Naddaf and S.Z. Heris, *J. Therm. Anal. Calorim.*, **135**, 1229 (2019); https://doi.org/10.1007/s10973-018-7456-8
47. H. Pourpasha, S.Z. Heris and A. Asadi, *J. Therm. Anal. Calorim.*, **138**, 57 (2019); https://doi.org/10.1007/s10973-019-08155-2
48. S.B. Mousavi and S.Z. Heris, *Int. J. Hydrogen Energy*, **45**, 23603 (2020); https://doi.org/10.1016/j.ijhydene.2020.05.259
49. A.M. Elsaid, *Int. Commun. Heat Mass Transfer*, **108**, 104263 (2019); https://doi.org/10.1016/j.icheatmasstransfer.2019.05.009
50. M.H. Esfe, A.A.A. Arani, S. Esfandeh and M. Afrand, *Energy*, **170**, 228 (2019); https://doi.org/10.1016/j.energy.2018.12.127
51. M.H. Esfe, A.A.A. Arani and S. Esfandeh, *Appl. Therm. Eng.*, **143**, 493 (2018); https://doi.org/10.1016/j.applthermaleng.2018.07.034
52. J. Zhong, J. Li, Z. Xiao, W. Hu, X. Zhou and X. Zheng, *Mater. Lett.*, **91**, 301 (2013); https://doi.org/10.1016/j.matlet.2012.10.040